Investigating Circular Dorsal Ruffles through Varying Substrate Stiffness and Mathematical Modeling

Yukai Zeng,[†‡△] Tanny Lai,[‡△] Cheng Gee Koh,[§¶] Philip R. LeDuc,[†‖] and K.-H. Chiam[‡¶]

[†]Mechanical Engineering, Carnegie Mellon University, Pittsburgh, Pennsylvania; [‡]Biophysics Group, A*STAR Institute of High Performance Computing, Singapore; [§]School of Biological Sciences, Nanyang Technological University, Singapore; [¶]Mechanobiology Institute, National University of Singapore, Singapore; and [‖]Biomedical Engineering, Computational Biology, and Biological Sciences, Carnegie Mellon University, Pittsburgh, Pennsylvania

Supporting Material

October 3, 2011

1 More cells exhibit CDRs when seeded on softer substrates

The percentage of cells in a sample which exhibited CDRs in a cell population was calculated by manually observing at least 500 cells in the given sample and counting the number of cells which had CDRs, and taking it as a percentage of the total number of observed cells in the sample. We found that by changing the substrate stiffness, we were able to modify the percentage of cells exhibiting CDRs, with more cells showing CDRs when seeded on less stiff substrates. This is quantified in Fig. S1 with a maximum of cells expressing CDRs within 5 min of stimulation and then slowly returning back to no CDR expression within 45 min. Based on observation of the signalling pathway depicted in Fig. 4 of the manuscript, we postulate that increasing the substrate stiffness leads to an increase in FAK concentration which might hinder the initial dissociation of stress fibers which have been shown to accompany CDR formation, therefore reducing the chance of CDR formation in cells. Yet, once CDR formation is achieved, the lifetime of CDR is prolonged by the increased replenishing of actin monomers resulting from heightened stress fiber formation on stiffer substrates prior to PDGF stimulation.

2 More F-actin detected in cells seeded on stiffer substrates prior to PDGF stimulation

Cells were costained for G-actin and F-actin with DNase I (Alexa Fluor 488; 2 μM) and phalloidin (Alexa Fluor 568; 6 μM) respectively for 60 min and imaged using an inverted fluorescent microscope (Zeiss, Axiovert 200) with a 63x (1.4 Numerical Aperture) objective. Using ImageJ, the ratio of the F-actin fluorescence intensity to the total actin fluorescence intensity (F-actin

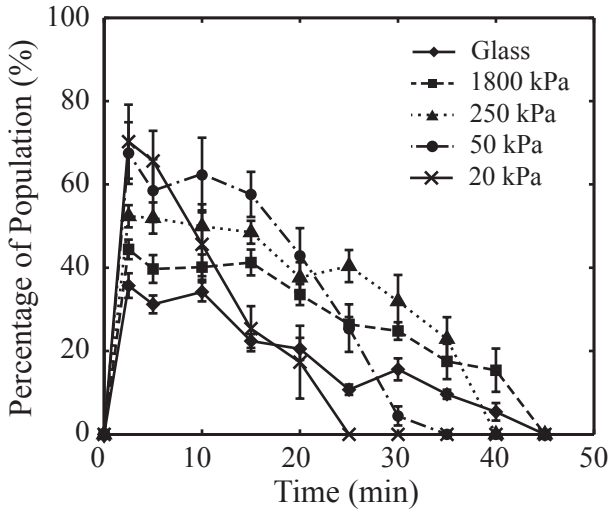

Figure S1: Percentage of cell population exhibiting CDRs versus time for PDMS substrates of different elasticities and glass substrates. (n=3). The bars denote one standard error.

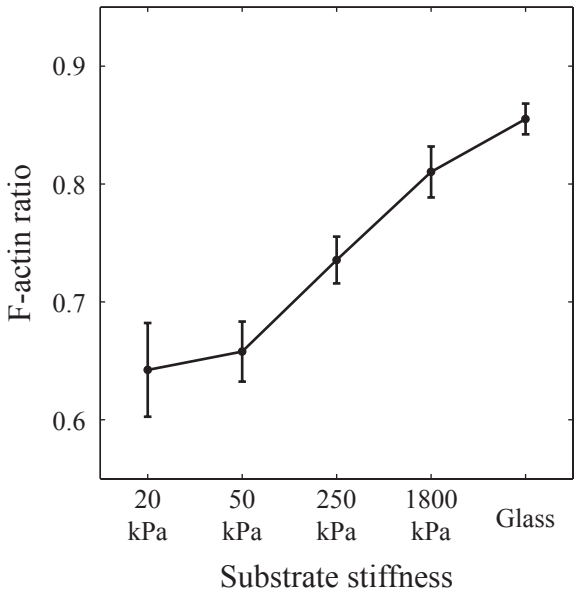

Figure S2: F-actin ratio for varying substrate stiffnesses. The bars denote one standard error.

and G-actin combined) in each cell was calculated. This ratio was averaged over 50 cells seeded on each substrate stiffness and the results are plotted in Fig. S2. The results show that increasing the substrate stiffness increases the ratio of actin incorporated in F-actin before PDGF stimulation.

3 Full mathematical model of proteins/lipids

This section documents the reactions between the different protein and lipid species involved in a potential pathway activated by the platelet-derived growth factor. The reactions are then converted into mathematical equations (referred to as reaction terms). The species are evolved under the effects of diffusion and the reaction terms in MATLAB (The Mathworks, Inc., Natick, MA). Cpt : Compartment; Rxn : Reaction. The subscripts a, c, and d refer to the active, cytosolic (inactive) and dorsal ruffle associated forms of the proteins respectively. Note that k_{-8} is a function of active myosin light chain and cofilin concentrations.

3.1 Abbreviations

Abbreviation	Definition
PDGF	Platelet-derived growth factor
PDGFR	Platelet-derived growth factor receptor
PI–3K	Phosphatidylinositol 3-kinase
PIP_2	Phosphatidylinositol (4,5)-bisphosphate
PIP_3	Phosphatidylinositol (3,4,5)-bisphosphate
RacGEF	Rac guanine exchange factor
RacGAP	Rac GTPase activating protein
RhoGEF	Rho guanine exchange factor
RhoGAP	Rho GTPase activating protein

ROCK	Rho-associated protein kinase
LIMK	LIM kinase
Cof	Cofilin
MLC	Myosin light chain
MLCP	Myosin light chain phosphatase
MLCP-P	Phosphorylated (inactive) myosin light chain phosphatase
MLCK	Myosin light chain kinase
F–actin	Stress fiber actin
G–actin	Monomeric actin
D–actin	Dorsal ruffle actin

3.2 Reactions

$$PDGF_2 + PDGFR \underset{k_{-1}}{\overset{k_1}{\rightleftharpoons}} PDGF_2\text{–}PDGFR \quad (1)$$

$$2PDGF_2\text{–}PDGFR \underset{k_{-2}}{\overset{k_2}{\rightleftharpoons}} PDGFR_a \quad (2)$$

$$PDGFR_a + PI\text{–}3K_c \xrightarrow{1} PDGFR_a + PI\text{–}3K_a \quad (3)$$

$$PI\text{–}3K_a + PIP_2 \xrightarrow{2} PI\text{–}3K_a + PIP_3 \quad (4)$$

$$PIP_2 + PTEN_c \underset{k_{-3}}{\overset{k_3}{\rightleftharpoons}} PTEN_a \quad (5)$$

$$PTEN_a + PIP_3 \xrightarrow{3} PTEN_a + PIP_2 \quad (6)$$

$$PIP_3 + RacGEF_c \underset{k_{-4}}{\overset{k_4}{\rightleftharpoons}} RacGEF_a \tag{7}$$

$$RacGEF_a + Rac_c \xrightarrow{4} RacGEF_a + Rac_a \tag{8}$$

$$WAVE1_c + Rac_a \underset{k_{-5}}{\overset{k_5}{\rightleftharpoons}} WAVE1_a \tag{9}$$

$$WAVE1_a + WGAP_c \xrightarrow{5} WAVE1_a + WGAP_a \tag{10}$$

$$WGAP_a + Rac_a \xrightarrow{6} WGAP_a + Rac_c \tag{11}$$

$$RhoA_a + ROCK \underset{k_{-6}}{\overset{k_6}{\rightleftharpoons}} ROCK_a \tag{12}$$

$$ROCK_a + LIMK_c \xrightarrow{7} ROCK_a + LIMK_a \tag{13}$$

$$LIMK_a + Cof_a \xrightarrow{8} LIMK_a + Cof_c \tag{14}$$

$$RhoA_a + mDia_c \underset{k_{-7}}{\overset{k_7}{\rightleftharpoons}} mDia_a \tag{15}$$

$$G\text{–}actin + mDia_a \underset{k_{-8}}{\overset{k_8}{\rightleftharpoons}} F\text{–}actin \tag{16}$$

$$WAVE1_a + Arp2/3 \underset{k_{-9}}{\overset{k_9}{\rightleftharpoons}} Arp2/3_d \tag{17}$$

$$Arp2/3_d + G\text{–}actin \underset{k_{-10}}{\overset{k_{10}}{\rightleftharpoons}} D\text{–}actin \tag{18}$$

$$ROCK_a + MLCP \xrightarrow{9} ROCK_a + MLCP\text{–}P \tag{19}$$

$$MLCP + MLC_a \xrightarrow{10} MLCP + MLC_c \tag{20}$$

$$MLCK + MLC_c \xrightarrow{11} MLCK + MLC_a \tag{21}$$

$$FAK_{pi} + RhoGEF \underset{k_{-11}}{\overset{k_{11}}{\rightleftharpoons}} RhoGEF_a \tag{22}$$

$$RhoA_c + RhoGEF_a \xrightarrow{12} RhoA_a + RhoGEF_a \tag{23}$$

$$ROCK_a + RacGAP_c \xrightarrow{13} ROCK_a + RacGAP_a \tag{24}$$

$$RacGAP_a + Rac_a \xrightarrow{14} RacGAP_a + Rac_c \tag{25}$$

$$Rac_a + RhoGAP_c \underset{k_{-12}}{\overset{k_{12}}{\rightleftharpoons}} RhoGAP_a \tag{26}$$

$$RhoGAP_a + RhoA_a \xrightarrow{15} RhoGAP_a + RhoA_c \qquad (27)$$

3.3 Equations

No	Cpt	Name	Reaction terms
1	e	$PDGF_2$	$-k_1[PDGF_2][PDGFR] + k_{-1}[PDGF_2\text{–}PDGFR]$
2	m	PDGFR	$-k_1[PDGF_2][PDGFR] + k_{-1}[PDGF_2\text{–}PDGFR]$
3	m	$PDGF_2$–PDGFR	$k_1[PDGF_2][PDGFR] - k_{-1}[PDGF_2\text{–}PDGFR] - k_2[PDGF_2\text{–}PDGFR]^2 + k_{-2}[PDGFR_a]$
4	m	$PDGFR_a$	$k_2[PDGF_2\text{–}PDGFR]^2 - k_{-2}[PDGFR_a]$
5	c	PI–$3K_c$	$-\frac{k_{cat,1}[PDGFR_a][PI\text{–}3K_c]}{k_{m1} + [PI\text{–}3K_c]}$
6	m	PI–$3K_a$	$\frac{k_{cat,1}[PDGFR_a][PI\text{–}3K_c]}{k_{m1} + [PI\text{–}3K_c]}$
7	m	PIP_2	$-\frac{k_{cat,2}[PI\text{–}3K_a][PIP_2]}{k_{m2} + [PIP_2]} + \frac{k_{cat,3}[PTEN_a][PIP_3]}{k_{m3} + [PIP_3]} - k_3[PIP_2][PTEN_c] + k_{-3}[PTEN_a]$
8	m	PIP_3	$\frac{k_{cat,2}[PI\text{–}3K_a][PIP_2]}{k_{m2} + [PIP_2]} - \frac{k_{cat,3}[PTEN_a][PIP_3]}{k_{m3} + [PIP_3]} - k_4[PIP_3][RacGEF_c] + k_{-4}[RacGEF_a]$

9	c	PTEN$_c$	$-k_3[PIP_2][PTEN_c] + k_{-3}[PTEN_a]$
10	m	PTEN$_a$	$k_3[PIP_2][PTEN_c] - k_{-3}[PTEN_a]$
11	c	RacGEF$_c$	$-k_4[RacGEF_c][PIP_3] + k_{-4}[RacGEF_a]$
12	m	RacGEF$_a$	$k_4[RacGEF_c][PIP_3] - k_{-4}[RacGEF_a]$
13	c	Rac$_c$	$-\frac{k_{cat,4}[RacGEF_a][Rac_c]}{k_{m4}+[Rac_c]} + \frac{k_{cat,6}[WGAP_a][Rac_a]}{k_{m6}+[Rac_a]} + \frac{k_{cat,14}[RacGAP_a][Rac_a]}{k_{m14}+[Rac_a]}$
14	m	Rac$_a$	$\frac{k_{cat,4}[RacGEF_a][Rac_c]}{k_{m4}+[Rac_c]} - \frac{k_{cat,6}[WGAP_a][Rac_a]}{k_{m6}+[Rac_a]} - \frac{k_{cat,14}[RacGAP_a][Rac_a]}{k_{m14}+[Rac_a]} - k_5[WAVE1_c][Rac_a] + k_{-5}[WAVE1_a] - k_{12}[RhoGAP_c][Rac_a] + k_{-12}[RhoGAP_a]$
15	c	WAVE1$_c$	$-k_5[WAVE1_c][Rac_a] + k_{-5}[WAVE1_a]$
16	m	WAVE1$_a$	$k_5[WAVE1_c][Rac_a] - k_{-5}[WAVE1_a] - k_9[WAVE1_a][Arp2/3] + k_{-9}[Arp2/3_d]$
17	c	WGAP$_c$	$-\frac{k_{cat,5}[WAVE1_a][WGAP_c]}{k_{m5}+[WGAP_c]}$
18	m	WGAP$_a$	$\frac{k_{cat,5}[WAVE1_a][WGAP_c]}{k_{m5}+[WGAP_c]}$

19	c	RhoGAP$_c$	$-k_{12}[RhoGAP_c][Rac_a] + k_{-12}[RhoGAP_a]$
20	m	RhoGAP$_a$	$k_{12}[RhoGAP_c][Rac_a] - k_{-12}[RhoGAP_a]$
21	c	RhoA$_a$	$-\frac{k_{cat,15}[RhoGAP_a][RhoA_a]}{k_{m15}+[RhoA_a]} + \frac{k_{cat,12}[RhoGEF_a][RhoA_c]}{k_{m12}+[RhoA_c]} - k_6[RhoA_a][ROCK] + k_{-6}[ROCK_a] - k_7[RhoA_a][mDia_c] + k_{-7}[mDia_a]$
22	c	RhoA$_c$	$\frac{k_{cat,15}[RhoGAP_a][RhoA_a]}{k_{m15}+[RhoA_a]} - \frac{k_{cat,12}[RhoGEF_a][RhoA_c]}{k_{m12}+[RhoA_c]}$
23	c	ROCK	$-k_6[RhoA_a][ROCK] + k_{-6}[ROCK_a]$
24	c	ROCK$_a$	$k_6[RhoA_a][ROCK] - k_{-6}[ROCK_a]$
25	c	LIMK$_c$	$-\frac{k_{cat,7}[ROCK_a][LIMK_c]}{k_{m7}+[LIMK_c]}$
26	c	LIMK$_a$	$\frac{k_{cat,7}[ROCK_a][LIMK_c]}{k_{m7}+[LIMK_c]}$
27	c	Cof$_a$	$-\frac{k_{cat,8}[LIMK_a][Cof_a]}{k_{m8}+[Cof_a]}$
28	c	Cof$_c$	$\frac{k_{cat,8}[LIMK_a][Cof_a]}{k_{m8}+[Cof_a]}$
29	c	mDia$_c$	$-k_7[RhoA_a][mDia_c] + k_{-7}[mDia_a]$

30	c	mDia$_a$	$k_7[RhoA_a][mDia_c] - k_{-8}[mDia_a] - k_8[G\text{–}actin][mDia_a] + k_{-8}[F\text{–}actin]$
31	c	MLCP	$-\frac{k_{cat,9}[ROCK_a][MLCP]}{k_{m9}+[MLCP]}$
32	c	MLCP–P	$\frac{k_{cat,9}[ROCK_a][MLCP]}{k_{m9}+[MLCP]}$
33	c	MLC$_a$	$-\frac{k_{cat,10}[MLCP][MLC_a]}{k_{m10}+[MLC_a]}+\frac{k_{cat,11}[MLCK][MLC_c]}{k_{m11}+[MLC_c]}$
34	c	MLC$_c$	$\frac{k_{cat,10}[MLCP][MLC_a]}{k_{m10}+[MLC_a]}-\frac{k_{cat,11}[MLCK][MLC_c]}{k_{m11}+[MLC_c]}$
35	c	G–actin	$-k_8[G\text{–}actin][mDia_a] + k_{-8}[F\text{–}actin] - k_{10}[Arp2/3_d][G\text{–}actin] + k_{-10}[D\text{–}actin]$
36	m	F–actin	$k_8[G\text{–}actin][mDia_a] - k_{-8}[F\text{–}actin]$
37	m	D–actin	$k_{10}[Arp2/3_d][G\text{–}actin] - k_{-10}[D\text{–}actin]$
38	c	Arp2/3	$-k_9[WAVE1_a][Arp2/3] + k_{-9}[Arp2/3_d]$
39	m	Arp2/3$_d$	$k_9[WAVE1_a][Arp2/3] - k_{-9}[Arp2/3_d] - k_{10}[Arp2/3_d][G\text{–}actin] + k_{-10}[D\text{–}actin]$
40	c	RhoGEF	$-k_{11}[FAK_{pi}][RhoGEF] + k_{-11}[RhoGEF_a]$

41	c	RhoGEF_a	$k_{11}[FAK_{pi}][RhoGEF] - k_{-11}[RhoGEF_a]$
42	c	RacGAP_c	$-\frac{k_{cat,13}[ROCK_a][RacGAP_c]}{k_{m13}+[RacGAP_c]}$
43	c	RacGAP_a	$\frac{k_{cat,13}[ROCK_a][RacGAP_c]}{k_{m13}+[RacGAP_c]}$

3.4 Parameters

Rxn	Parameters	Values	References
1	k_1 , k_{-1}	0.7 nM^{-1} s^{-1} , 1.0 s^{-1}	Park et al (1)
2	k_2 , k_{-2}	0.122 μM^{-1} s^{-1} , 0.00122 s^{-1}	Park et al (1)
3	$k_{cat,1}$, k_{m1}	1.0 s^{-1} , 100 nM	Estimated
4	$k_{cat,2}$, k_{m2}	1.0 s^{-1} , 200 nM	Gamba et al (2), Naoki et al (3)
5	k_3 , k_{-3}	50 μM^{-1} s^{-1} , 0.1 s^{-1}	Gamba et al (2)
6	$k_{cat,3}$, k_{m3}	0.5 s^{-1} , 200 nM	Gamba et al (2), Naoki et al (3)
7	k_4 , k_{-4}	5 μM^{-1} s^{-1} , 50 s^{-1}	Naoki et al (3)
8	$k_{cat,4}$, k_{m4}	1.0 s^{-1} , 100 nM	Naoki et al (3)
9	k_5 , k_{-5}	1 μM^{-1} s^{-1} , 1 s^{-1}	Estimated
10	$k_{cat,5}$, k_{m5}	1.0 s^{-1} , 100 nM	Estimated

11	$k_{cat,6}$, k_{m6}	0.1 s^{-1} , 10 nM	Naoki et al (3)
12	k_6 , k_{-6}	1 μM^{-1} s^{-1} , 1 s^{-1}	Estimated
13	$k_{cat,7}$, k_{m7}	2 s^{-1} , 3.1 μM	Turner et al (4)
14	$k_{cat,8}$, k_{m8}	1 s^{-1} , 1 μM	Sakumura et al (5)
15	k_7 , k_{-7}	0.5 μM^{-1} s^{-1} , 0.003 s^{-1}	Lammers et al (6)
16	k_8	1 μM^{-1} s^{-1}	Estimated
17	k_9 , k_{-9}	1 μM^{-1} s^{-1} , 1 s^{-1}	Estimated
18	k_{10} , k_{-10}	1 μM^{-1} s^{-1} , 1 s^{-1}	Estimated
19	$k_{cat,9}$, k_{m9}	2.4 s^{-1} , 0.1 μM	Besser et al (7)
20	$k_{cat,10}$, k_{m10}	21 s^{-1} , 10 μM	Besser et al (7)
21	$k_{cat,11}$, k_{m11}	10 s^{-1} , 20 μM	Besser et al (7)
22	k_{11} , k_{-11}	1 μM^{-1} s^{-1} , 1 s^{-1}	Estimated
23	$k_{cat,12}$, k_{m12}	1 s^{-1} , 1 μM	Estimated
24	$k_{cat,13}$, k_{m13}	1 s^{-1} , 1 μM	Estimated
25	$k_{cat,14}$, k_{m14}	1 s^{-1} , 1 μM	Estimated
26	k_{12} , k_{-12}	1 μM^{-1} s^{-1} , 1 s^{-1}	Estimated
27	$k_{cat,15}$, k_{m15}	1 s^{-1} , 1 μM	Estimated

4 Analysis of the reduced model

The nullclines of active Rac and active WGAP were obtained by solving the steady state solutions of the reduced model. Observation of the phase plane in Fig. 7 tells us clearly that the steady state solution indicated by the star is a stable one. To achieve large excursions in the value of Rac when the system is moved out of its steady state, the value of WGAP must be sufficiently low. This critical value of WGAP is indicated by the largely unchanging portion of the Rac nullcline. Rearranging the terms in the equation $\partial x/\partial t = 0$, we obtain

$$y = \frac{v_1}{v_2}\left[1 + k_{m2}\frac{-x^2 - x + 1}{x^2(k_{m1} + 1 - x)}\right]$$

Given that the value of k_{m2} is small (note that k_{m2} governs the deactivation rate of Rac due to WGAP), the value of y can be approximated to be v_1/v_2. In the simulations, the ratio used was 0.5.

References

1. Park, C. S., I. C. Schneider, and J. M. Haugh, 2003. Kinetic analysis of platelet-derived growth factor receptor/phosphoinositide 3-kinase/Akt signaling in fibroblasts. *The Journal of biological chemistry* 278:37064–37072.

2. Gamba, A., A. de Candia, S. Di Talia, A. Coniglio, F. Bussolino, and G. Serini, 2005. Diffusion-limited phase separation in eukaryotic chemotaxis. *Proceedings of the National Academy of Sciences of the United States of America* 102:16927–16932.

3. Naoki, H., Y. Sakumura, and S. Ishii, 2008. Stochastic control of spontaneous signal generation for gradient sensing in chemotaxis. *Journal of theoretical biology* 255:259–266.

4. Turner, M. S., J. W. Trauger, J. Stephens, and P. LoGrasso, 2002. Characterization and purification of truncated human Rho-kinase II expressed in Sf-21 cells. *Archives of biochemistry and biophysics* 405:13–20.

5. Sakumura, Y., Y. Tsukada, N. Yamamoto, and S. Ishii, 2005. A molecular model for axon guidance based on cross talk between rho GTPases. *Biophysical journal* 89:812–822.

6. Lammers, M., S. Meyer, D. Kuhlmann, and A. Wittinghofer, 2008. Specificity of interactions between mDia isoforms and Rho proteins. *The Journal of biological chemistry* 283:35236–35246.

7. Besser, A., and U. S. Schwarz, 2007. Coupling biochemistry and mechanics in cell adhesion: a model for inhomogeneous stress fiber contraction. *New Journal of Physics* 9:425. `http://stacks.iop.org/1367-2630/9/i=11/a=425`.